

PrintPOWER – Paste systems for multifunctional copper power modules

K. Reinhardt, S. Körner, and U. Partsch

Fraunhofer Institute for Ceramic Technologies and Systems IKTS, Winterbergstraße 28, 01277 Dresden

+49 351 2553 7837, kathrin.reinhardt@ikts.fraunhofer.de

Abstract

The aim of the present work was the development of paste systems for use in the high temperature and low temperature range, which can be used for the construction of copper-based power electronic components. In doing so, a feasibility was to be elaborated which shows the combination and functionality of all paste systems, so that in future individual power modules can be set up. For this purpose, the following single-paste systems were developed or further developed: copper thick film pastes, glass insulations, silver polymer pastes and Al₂O₃ polymer insulation. To verify the compatibility of the individual developed paste systems, a printed multi-layer module was set up and the layers tested for functionality. It could be shown that the developed paste systems can be combined with each other and can be sintered or hardened under nitrogen atmosphere without suffering a loss of function. Accordingly, it is possible in the future to build application-related power modules with the previously developed paste systems.

Key words: Thick-film power modules, copper multilayer circuits, high temperature pastes, low temperature pastes, rheology, 3D dispensing

Introduction

Power electronic systems are the backbone of the energy transition and environmentally friendly individual electro mobility. Modules in which power semiconductors and other components are integrated form the heart of such systems. Copper thick films combine the advantages of DCB substrates, which are dominant in the module sector, and the silver thick-film technology used for highly reliable signal processing circuits. The focus of the work was the development of copper-compatible paste systems (conductive and dielectric pastes) and their combination to create multilayer module structures on ceramic substrates. The printed modules on the multifunctional substrates should be able to contain, in addition to the power semiconductors, various other active and passive components. This integrated functionality at the module level, let these modules count to the class of the “Intelligent Power Modules” (IPM).

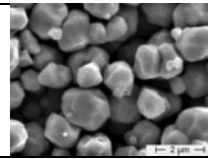
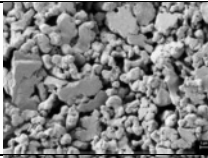
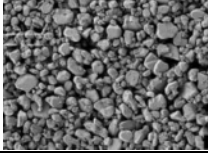
Experimental

A. Materials and Paste Preparation

For the development of high-temperature (HT) and low-temperature (LT) suspensions, the materials listed in Table 1 were used as inorganic main components. For the HT copper metallizations the inorganic powders were mixed together in a roller bench for 25 min. The mixture was ground together in a dissolver with a solution of polyacrylate in texanol. The pre-dispersed suspensions were finally homogenized using a three-

roll mill (EXAKT 120E). The HT glass isolation as well as the LT suspensions (Ag metallization and Al₂O₃ isolation) were comparable formulated. The inorganic powders were dispersed in polymer solutions (HT isolation: polyacrylate/texanol solution; LT suspensions: PVB/Terpineol solutions) in a SpeedMixer™ (DAC 150 FVZ Hauschild & Co. KG) and after this also homogenized using a three-roll mill.

Table 1: Investigated suspensions depending on the inorganic main component.

Type of suspension	Inorganic main component	FESEM image
HT metallization	Copper	
HT isolation	Glass	---
LT metallization	Silver	
LT isolation	Alumina	

B. Printing Tests

All HT suspensions and the LT insulation suspension were screen printed. The printing tests were carried out on a screen printer Microtronic II from EKRA. The characterization layout for the HT Cu suspensions is shown in figure 1a) and for the HT glass and LT polymer suspensions in figure 1b).

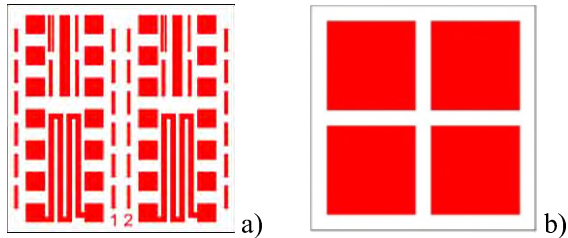


Figure 1: Screen-Printing test layouts for a) HT Cu suspensions, b) HT glass and LT Al_2O_3 insulations.

The LT silver suspensions were deposited on a dispenser from Asymtek, Axiom 1000 X-1010.

For the demonstrator a test layout shown in figure 2 was used, where the feasibility of the combination of all pastes for using in a power module were tested.

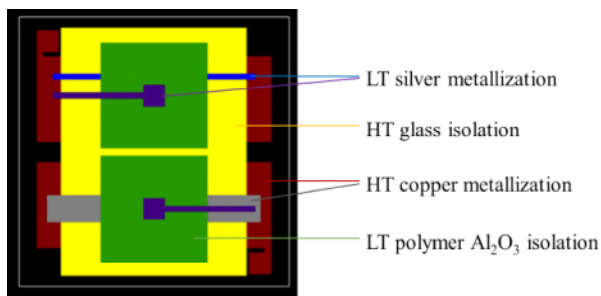


Figure 2: Demonstrator test layout for printed power electronics modules.

C. Electrical and mechanical characterization:

The following investigations were carried out on the deposited layers:

- Electrical (resistance measurements) and
 - Mechanical characterization (wire-peel, pull stud and tesaband test)
- fired and hardened layers (including aging tests such as thermal aging (150 °C, 100 h).

Results and Discussions

A. HT copper metallization

The main aim for HT copper metallization was the further development of the copper paste system with regard to achieve higher aspect ratios for higher conductivity. For this different surfactants were tested which should improve the printing resolution. Therefore, it is necessary to use additives, which burn out under nitrogen atmosphere

without any residue. The results of the following three copper pastes are presented:

- Cu paste A: without any surfactant,
- Cu paste B: with surfactant I (softener),
- Cu paste C: with surfactant II (surface additive).

All copper layers were fired at 955 °C for 15 minutes under nitrogen atmosphere in a belt furnace. An overview of the printing qualities and the reached aspect ratios ($\text{AR} = \text{Height} / \text{Line width}$) is compiled in figure 3. The addition of additives allows an increase in the layer thickness and a reduction in the line width. It can be seen that the Cu paste C with the surface additive achieves the highest aspect ratio (0.21), whereas the omissions of additives results in a very low aspect ratio (Cu paste A, $\text{AR} = 0.05$). This shows that the addition of additives can be used specifically for setting geometric line properties. Direct control is possible. However, an improvement in the aspect ratio results in a deterioration of the surface quality, so that for the Cu paste C a light screen structure can be observed.

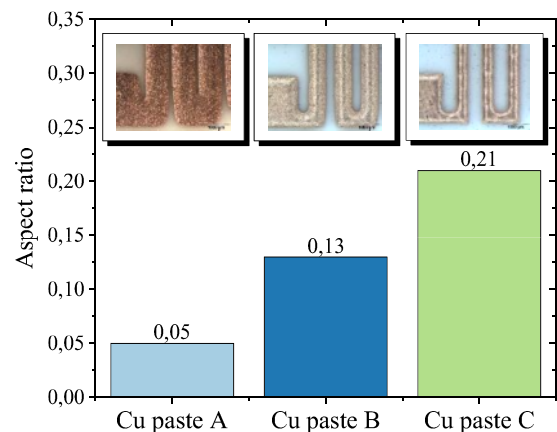


Figure 3: Aspect ratios of the examined HT Cu metallizations with and without surfactant addition on Al_2O_3 substrates, including microscopic pictures.

The Cu pastes were also evaluated for their electrical conductivity (Figure 4). By adding additives, the electrical conductivity could be increased. Thus, an increase of 430 kS/cm for Cu paste A to 451.4 kS/cm was achieved for Cu paste C, which corresponds to 77.8 % of the Cu bulk resistance. This increase can be explained on the one hand with the improvement of the aspect ratio of the printed layers, on the other hand, the addition of additive allows an increase in the solids content. Thus, for Cu paste A only a maximum solids content of 85 % was achieved, whereas Cu paste B contains 88 % solids and Cu paste C 89 %. The reduction in conductivity despite increasing the solids content for Cu paste B may possibly be explained by incomplete burnout of the additive during the nitrogen-firing step. Carbon residues can negatively affect the

sintering behavior and increase the electrical resistance of the layer.

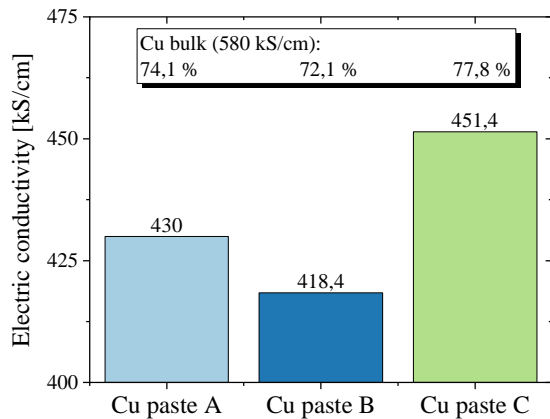


Figure 4: Electric conductivity of the examined HT Cu metallizations with and without surfactant addition on Al₂O₃ substrates.

The mechanical adhesion of the layers was characterized by wire peel test. In this case, the adhesion of the sintered layer to the substrate is not measured directly, but the adhesion of a soldered connection to a sintered layer is measured. Figure 5 compares the results for the three HT Cu suspensions. The measurements being carried out initially after firing and after an aging of 100 h at 150 °C. It can be observed that the adhesive strength increases with increasing solids content. For the Cu paste C a maximum adhesion of 30.8 N/4mm² are achieved. With the exception of Cu paste B, the characterized pastes show no reduction in adhesive strength after aging at 150 °C. for 100 h. Again, the decrease in adhesion of Cu paste B after the aging step can be explained with possible carbon residues within the layer, which could reduce the layer properties. This indicates that the surfactants can probably influence the microstructure on the surface of the Cu layers (connection to the solder) or at the interface to the Al₂O₃ substrate. So the adhesion can be specific adjust.

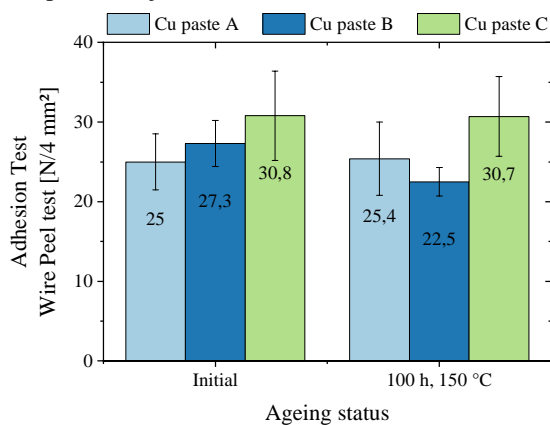


Figure 5: Wire-peel test results of the examined HT Cu metallizations with and without surfactant addition on Al₂O₃ substrates.

In conclusion can be said that varying the composition of copper pastes, in particular with rheological additives, it was possible to specifically set different layer geometries, different conductivities and different adhesion behaviors.

B. HT glass isolation

For the isolation of the HT Cu layers two different glasses were selected, one commercial (glass I) and one IKTS glass (glass II). First, they were tested on whether they can be sintered under a nitrogen atmosphere, so that forms a firm, defect-free layer and no reactions with the copper layers occur. Table 2 compares the sintered layers of the HT glass insulation suspensions of glass I and II as a function of the sintering end temperature on non-printed Al₂O₃ substrates and printed HT Cu layers (Cu paste A).

Table 2: Overview of screen printing qualities of HT glass insulations (glass I & II) on non-printed Al₂O₃ substrates and printed HT Cu layers.

Type of suspension	850 °C, 15 min, N ₂	955 °C, 15 min, N ₂
Glass I on Al ₂ O ₃ blank		
Glass I on Cu paste A		
Glass II on Al ₂ O ₃ blank		
Glass II on Cu paste A		

The glass I suspension shows glazed sintered layers on Al₂O₃ (row 2) irrespective of the sintering end temperature, which have a light gray color. The gray coloration can be attributed to small carbon residues within the glass layer, which probably occur during the nitrogen burn-out of the polymer solution. Nevertheless it do not prevent the sintering

behavior of the glass layer. Whitish stains within the glass layers may possibly indicate dewetting or poor leveling behavior of the suspension on the substrate surface. If the glass I suspension is applied to the HT Cu layer and sintered (row 3), interactions occur in the form of bubble formation between the glass insulation and the Cu layer as the sintering end temperature increases. A maximum sintering temperature of 850 °C is therefore possible for the glass I suspension on HT Cu layers.

The glass II suspension has a matt glass surface on Al₂O₃ (row 4) for a final sintering temperature of 850 °C., which forms a glassy transparent layer only at a sintering temperature of 955 °C. This shows that for the sintering of the glass II a temperature of 955 °C is necessary to form a dense insulation layer. Furthermore a strong surface structure can be established, which can be explained here due to the lower viscosity of the glass suspension (due to the chosen polymer solution). A comparable image is observed for the printing of the glass II suspension onto the HT Cu layer (row 5). Again, only a glassy, transparent layer is formed at a sintering temperature of 955 °C. Furthermore, no significant interactions of the glass insulation with the Cu layer can be occur.

The HT glass insulation layers were tested for their mechanical adhesion on Al₂O₃ and on the HT Cu metallizations. The pull stud test was carried out, in which the adhesion forces between the layers are measured directly by means of an epoxy stamped aluminum stud. For the test, the following samples were selected, which showed the best sintering results:

- Glass I: 850 °C, 15 min, N₂
- Glass II: 955 °C, 15 min, N₂

Figure 6 compares the results of the pull stud test of the selected samples. The glass insulation layers on blank Al₂O₃ show maximum adhesion values between 465 N/5.73mm² and 523 N/5.73mm², without any ageing cycle. The highest adhesion to Al₂O₃ can be observed for the glass I insulation, which was sintered at 850 °C. It was also possible to observe predominantly ceramic fracture for all layers on Al₂O₃ as the fracture pattern, that means the weakest point in this layer composite is the Al₂O₃ ceramic and high adhesive properties of the glass insulations can be assumed.

Comparing the results presented above with the adhesion tests of the glass insulations on HT Cu layers, the adhesion values for all glass insulations are reduced, but to varying degrees depending on the respective glass insulation. For the glass I insulations a significantly greater decrease in adhesive strength is occurred, which decreases by more than 65% (162 N/5.73mm²). The glass II insulation has a 34% percent reduction, but has the highest adhesive properties on HT Cu layers (306 N/5.73mm²) compared to all other glass insulations. The fracture pattern of the glass

insulation on Cu layers is not like for the pure Al₂O₃ substrates predominantly ceramic fracture, but the aluminum stamp triggers in the peel test above all the glass layer, the Cu layer still adhered to the substrate. This could be determined for all examined samples.

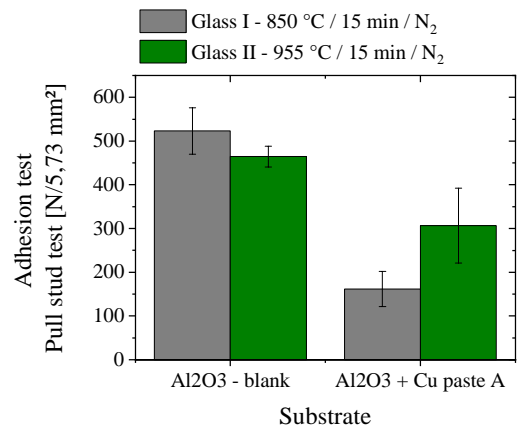


Figure 6: Pull stud test results of the investigated HT glass insulations on non-printed Al₂O₃ substrates and printed HT Cu layers.

In conclusion, it can be said that a direct relationship to the sintering end temperature cannot be found with the samples selected here, but a clear difference with respect to the underlying layer of the glass insulation.

C. LT silver metallization

To replace wire bonding in later power electronic components, polymer based pastes will be evaluated. These can be deposited in addition to the screen printing, inter alia, with 3D substrate compatible deposition methods such as dispense jetting. For the LT Ag metallizations one silver powder was tested which was mixed in two different PVB polymer solutions. A short-chain (Ag paste A) and a longer-chain polymer (Ag paste B) was selected. The silver pastes were deposited by dispense jetting on Al₂O₃ substrates with prefabricated contact pads. This was followed by a variation of the curing temperature and curing time for both pastes and a subsequent electrical characterization.

Figure 7 shows the dependence of the sheet resistance on the curing conditions of the LT Ag pastes A and B. As the thermal input increases, the resistance of the functional layers decreases. The Ag paste B layers tend to have a lower resistance (8.2 mOhm/sq @ 280°C for 30 min) than the Ag paste A layers (9.2 mOhm/sq @ 280°C for 30 min) - this is a result of the slightly higher silver content in the hardened layers of the Ag paste A. With regard to a further lowering of the sheet resistance, current work focuses on a variation of the silver powder and an optimization of the binder system in order to improve curing conditions to lower temperatures and times. Sheet resistance less than 6 mOhm/sq can be

observed for curing conditions of 200 °C for 10 minutes.

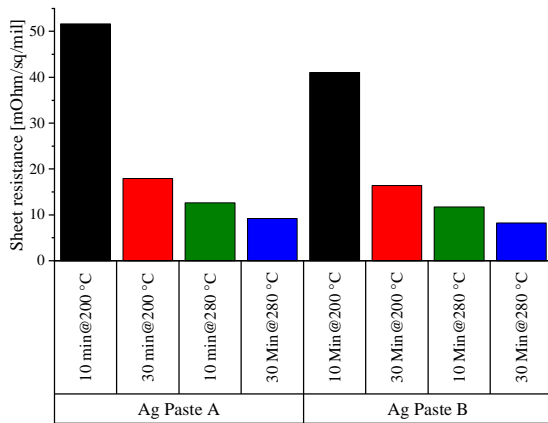


Figure 7: Sheet resistance of LT Ag pastes A and B depending on the curing conditions.

D. LT polymer Al₂O₃ isolation

The functionality of the insulation layers was demonstrated by measuring the insulating resistance and breakdown voltage. Figure 8 shows the insulation resistance (columns) and the associated breakdown voltage (symbols) of the polymer-based Al₂O₃ insulation paste as a function of the extent of the aging of the suspension (black - initial measurement after layer hardening, red - aging for 500 h at 150 °C, blue - aging for 500 h at 85 °C and 85 % relative humidity). The test structures were first built up by screen printing. As electrodes for the power supply, the silver polymer pastes developed in the project were used. The characteristic values of the initial measurement for the insulation resistance are in the range of 4.1E12 ohms - the pertinent breakdown voltage is 1000 V. The aging of the samples at 150 °C for 500 h causes the insulation resistance to increase again to 4E13 ohms - compared to the initial ones the breakdown voltage remains constant at 1000 V. The increase in the insulation resistance can either be an indication that the layers were initially not completely cured or that the polymer absorbs humidity, which was removed by the long removal time at 150 °C and so on the insulation resistance increases. An indication of the second possibility shows the aging at 85 °C and 85 % relative humidity. After a storage time of 500 h, the insulation resistance drops to 2.2E10 ohms and the breakdown voltage drops to 488 V (without sample 3, with sample 3 to 570 V). Whether this process is reversible or can be reduced by adjusting the parameters during initial hardening remains to be investigated.

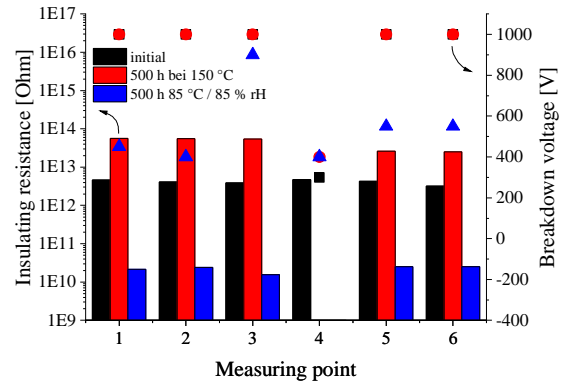


Figure 8: Insulation resistance (columns) and associated breakdown voltage (symbols) of the polymer-based Al₂O₃ insulation paste depending on the aging condition: black - initial measurement after layer hardening, red - aging for 500 h at 150 °C, blue - aging for 500 h at 85 °C and 85 % relative humidity.

E. Demonstrator

For demonstration purposes and to verify the compatibility of the developed paste systems, a multi-layer module was printed and various functional tests were performed. For the demonstrator setup, the following suspensions were selected:

- HT Cu metallization: Cu paste A (without surfactants)
- HT glass insulation: Glass paste I, sintering end temp.: 850 °C Glass paste II, sinter end temp.: 955 °C
- LT Ag metallization: Ag paste B
- LT polymer Al₂O₃ isolation.

The structure was based on the layout in figure 2. The printing order was chosen as follows:

- Print and firing first HT Cu metallization
- Print and firing HT glass insulation
- Print and firing second HT Cu metallization
- Print and curing first LT Ag metallization
- Print and curing LT polymer Al₂O₃ insulation
- Print and curing second LT Ag metallization.

It could be shown that the developed paste systems can be combined with each other and can be sintered or hardened under nitrogen atmosphere without suffering a loss of function (see figure 9). Accordingly, it is possible in the future to build application-oriented power modules with the previously developed paste systems.

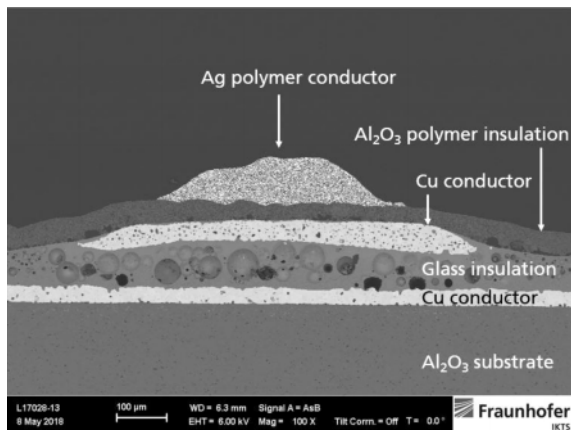


Figure 9: Cross-section of a printed multi-layer module demonstrator.

The characterization of the demonstrator was based on the measurement of sheet resistances between the individual metallizations. Figure 10 shows the demonstrator for the printed power electronics module with numbered measuring points for resistance determination. These are sintered copper pads (blue; Cu paste A), a sintered glass insulation (beige; glass I or II), a sintered copper conductor (red; Cu paste A) and a hardened silver conductor (gray; Ag paste B) and polymer-based insulation layer (green; Al₂O₃ paste). The sheet resistances of the HT Cu metallization (red interconnect structure Figure 10) and the LT Ag metallization (gray interconnect structure Figure 10) are shown in Figure 11. The resistors have not been normalized to a layer thickness.

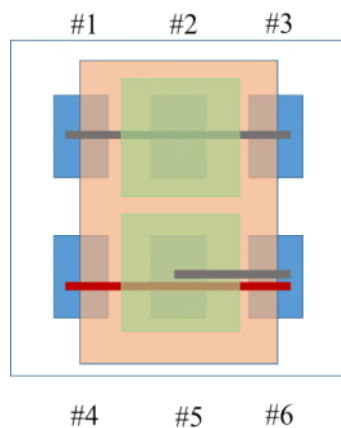


Figure 10: Demonstrator layout for printed power electronics modules with numbered measuring points for describing electrical resistance measurements.

The sheet resistance of the silver polymer paste B is 8.6 mOhm/sq (substrate Cu paste A / glass I) or 6.0 mOhm/sq (substrate Cu paste A / glass I, red columns) respectively lower than comparable curing conditions on test substrates (Figure 7). However, the hardening of the LT silver conductive path from # 1 to # 3 takes place in triplicate: initially after printing, a second time after the insulation layer

has been printed, and finally after the last print of the conductor from # 6 to # 5. Since the sheet resistance decreases with increasing thermal input of the paste, this difference can be explained. The difference between the two substrates is explained by the surface quality of the fired-glass insulations and the associated layer geometry of the silver guides. The sheet resistance between # 4 and # 5 is expected to be between that of the copper and the silver paste. The sheet resistances of the HT-Cu interconnects are 1.9 mOhm/sq (substrate Cu paste A / glass I) or 1.7 mOhm/sq (substrate Cu paste A / glass II, blue columns) in a resistance range that corresponds to the preliminary investigations.

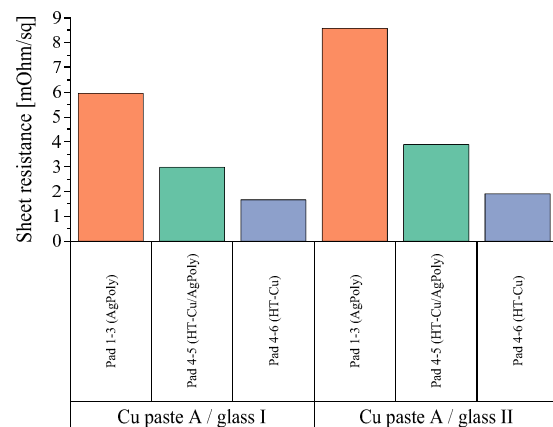


Figure 11: Sheet resistance of substrates Cu paste A / glass I and Cu paste A / glass II. red - sheet resistance Ag paste B from # 1 to # 3; green - sheet resistance Cu paste A / Ag paste B from # 4 to # 5; blue - sheet resistance Cu paste A from # 4 to # 6.

Conclusion

By using the developed copper thick film pastes and adapted insulation pastes for inert firing or curing, several functions can be embedded in power module structures. Furthermore, new contacting options were evaluated via 3D-printed silver polymer suspensions, which could replace established technologies, such as bonding or Siemens Planar Interconnect Technology (SiPLIT), and are more cost-effectively and with high reliability.

As part of these investigations, the following single paste-systems have been developed:

- Copper thick film pastes for thick print and fine line applications: By varying the composition of copper pastes, in particular with rheological additives, it was possible to specifically set different layer geometries, which enable both thick printing and fine line printing.
- Glass insulations for nitrogen atmospheres: Two glasses were evaluated which sinter densely and transparently at temperatures of up to 955 °C and have only small carbon residues within the layer. This makes it possible to use the developed glass pastes as dielectric layers, but

also as covering layers. Furthermore, the development of glass insulation for sintering temperatures ≥ 850 °C allows a multilayer structure with HT-Cu systems, so that robust circuits can be integrated in several levels.

- Silver polymer pastes: For the low temperature range, a silver metallization has been developed, which has very good conducting properties and can be deposited by means of dispensing printing processes. This will allow future use of new 3D contacting options that can replace established technologies such as bonding or the SiPLIT method more cost-effectively and with higher reliability.
- Al₂O₃ polymer insulation: In addition, an Al₂O₃ polymer insulation was developed, which has good insulation properties and can complete the assembly of a power multilayer module.